論文の内容の要旨

論文題目

Atomically Precise Gold Clusters Stabilized by Polyvinylpyrrolidone: Synthesis, Structural Analysis, and Catalysis

(ポリビニルピロリドン保護金クラスターの
原子精度合成、構造解析及び触媒作用)

氏名　長谷川　慎吾

1. Introduction

Metal clusters smaller than the critical dimension of ~2 nm are known to exhibit unique chemical properties which cannot be predicted from those of bulk and nanoparticles of corresponding metal [1,2]. To take full advantage of the size-specific chemical properties, it is essential to control the size with atomic precision. Atomically precise synthesis of Au clusters has been achieved by using protecting ligands such as thiolates, alkynyls, halides, phosphines, and *N*-heterocyclic carbenes [1,3]. Nevertheless, these ligand-protected Au clusters are in general catalytically inactive due to the capping of all the surface Au atoms. Stabilization by linear polymers is suitable for the catalytic applications of metal clusters, since the surface of clusters is inevitably exposed owing to the bulkiness of polymers [4]. It has been demonstrated that small (<3 nm) Au clusters stabilized by polyvinylpyrrolidone (PVP) show size-specific and high catalytic activities for oxidation reactions [5]. Major challenges for the studies of polymer-stabilized Au clusters are the atomically precise size control and determination of the atomic structure, because the post-synthetic isolation methods and X-ray crystallography are not applicable due to weak Au-polymer interactions and the polydisperse structure of polymer layers. In my doctoral study, I achieved the kinetically-controlled synthesis of new magic clusters of Au_{24}, $Au_{23}Pd_1$, and Au_{38} stabilized by PVP, as demonstrated by matrix-assisted laser desorption/ionization (MALDI) mass spectrometry. I investigated the structures of the clusters by aberration-corrected transmission electron microscopy (ACTEM), X-ray absorption spectroscopy (XAS), and

density functional theory (DFT) calculations. Based on the kinetic studies of aerobic oxidation of alcohols catalyzed by Au_{24}, $Au_{23}Pd_1$, and Au_{38}, doping and size effects on the catalysis are discussed.

2. Synthesis and Structural Analysis

In order to examine the effect of the amount of PVP on the cluster size, three samples **a**–**c** were prepared by mixing aqueous solutions of $HAuCl_4$ and $NaBH_4$ using a microfluidic mixer at the PVP/Au ratio of 40, 100, and 200, respectively. According to MALDI mass spectrometry, sample **a** contained Au_{34} and Au_{43}, whereas sample **b** was a mixture of Au_{24}, Au_{33}, and Au_{34}. Notably, sample **c** contained only Au_{24} (**Figure 1a**) and thus is referred to as Au_{24}:PVP, hereafter. Single Pd atom was successfully doped into Au_{24}:PVP by co-reduction of the mixture of $HAuCl_4$ and Na_2PdCl_4 with molar ratio of 23 : 1 (**Figure 1b**). On the other hand, it was found that Au_{38}:PVP was selectively obtained by the size conversion of the mixture of Au_{34} and Au_{43} (sample **a)** in basic aqueous solution (**Figure 1c**). Optical absorption spectroscopy, powder X-ray diffractometry, Au L_3-edge extended X-ray absorption fine structure (EXAFS) analysis, and ACTEM observation showed that the Au_{24}, $Au_{23}Pd_1$, and Au_{38} samples were not contaminated with Au nanoparticles larger than 2 nm.

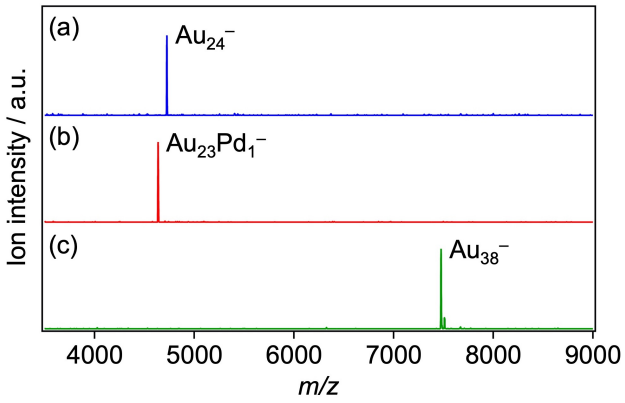

Figure 1. Negative-ion MALDI mass spectra of (a) Au_{24}:PVP, (b) $Au_{23}Pd_1$:PVP and (c) Au_{38}:PVP.

To confirm distinctive size difference between Au_{24}:PVP and Au_{38}:PVP and further obtain insights into atomic structures of the Au clusters, I conducted the structural analysis by ACTEM video imaging with fast imaging rate (25 images per second) and theoretical calculations. For the explanation of the observed ACTEM images, structural search of bare Au_{24} and Au_{38} clusters was carried out by DFT calculations. Both Au_{24} and Au_{38} showed non-crystalline structures (**Figures 2c** and **3c**) as stable isomers. Interestingly, all the constituent Au atoms of stable isomers of Au_{24} were exposed on the cluster surface. Simulated TEM images of these model structures obtained by multi-slice procedure qualitatively reproduced some of the ACTEM images of Au_{24}:PVP. Since different particles of Au_{24}:PVP were assigned to different model structures, it was revealed that the atomic structure of Au_{24}:PVP was polydisperse. Furthermore, ACTEM images of single particle of Au_{24}:PVP showed dynamic behavior, as illustrated in **Figure 2a**. The temporal change could not be explained by the rotation of single isomer but

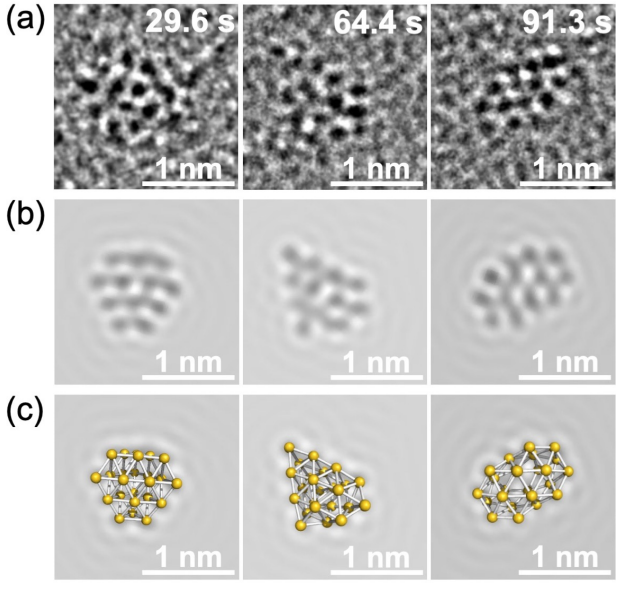

Figure 2. (a) ACTEM images of single particle of Au_{24}:PVP with time from the beginning of video recording. Corresponding (b) simulated images and (c) model structures.

by different isomers (**Figure 2c**). Therefore, it was found that the core structure of Au_{24}:PVP was fluxional due to the structural isomerization. Au_{38}:PVP also showed the polydisperse and dynamic core structure; ACTEM images of different particles of Au_{38}:PVP were assigned to different model structures and temporal change of single particle (**Figure 3a**) was ascribed to the interconversion between structural isomers (**Figure 3c**).

The local structure around the Pd atom of $Au_{23}Pd_1$:PVP was investigated by Pd K-edge EXAFS analysis, Fourier transform infrared (FT-IR) spectroscopy of adsorbed carbon monoxide, and DFT calculations. The Pd K-edge FT-EXAFS spectrum of $Au_{23}Pd_1$:PVP was dominated by the contribution of the Pd–Au bond (**Figure 4a**) and the coordination number (CN) was estimated to be 6.1 ± 0.7 by curve fitting analysis. The CN value significantly smaller than 12 indicated that the Pd atom is not confined within the Au cluster but exposed on the surface of the Au cluster, which was supported by the result of structural search of model $Au_{23}Pd_1$ cluster by DFT calculations. Several structural isomers with 6-coordinated Pd atoms were obtained as stable isomers.

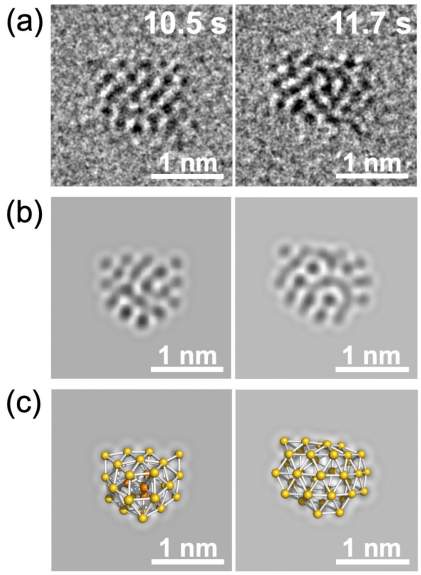

Figure 3. (a) ACTEM images of single particle of Au_{38}:PVP with time from the beginning of video recording. Corresponding (b) simulated images and (c) model structures.

The FT-IR spectrum of ^{12}CO-saturated colloidal solution of $Au_{23}Pd_1$:PVP showed two absorption bands at 2097 and 2038 cm^{-1} in addition to that of free CO at 2136 cm^{-1} (**Figure 4b**). These absorption bands were assigned to the stretching mode of CO adsorbed on the atop sites of Au and Pd atoms, respectively, according to the result for CO adsorbed on Au_{24}:PVP. These assignments were further supported by the DFT calculations on the CO adsorbed on structural isomers of $Au_{23}Pd_1$. Calculated frequencies of CO did not significantly depend on the structure of the clusters but primarily depended on the element of the adsorption sites (**Figure 4b**). Since the model $Au_{23}Pd_1(CO)_1$ cluster with a Pd atom encapsulated by Au atoms showed only one absorption band at ~2100 cm^{-1}, the appearance of two absorption bands in the FT-IR spectrum supported the proposed structure of $Au_{23}Pd_1$:PVP where the Pd dopant was exposed.

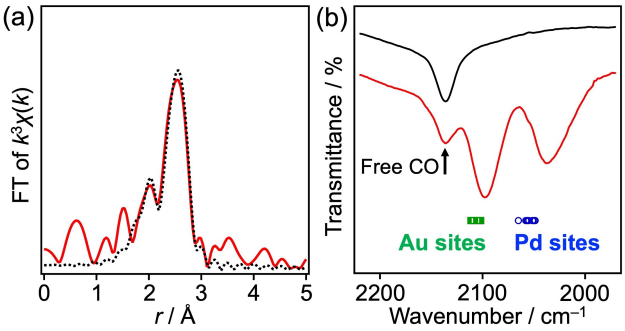

Figure 4. (a) Pd K-edge FT-EXAFS spectrum of $Au_{23}Pd_1$:PVP (solid) and fitting curve (dotted). (b) FT-IR spectra of ^{12}CO-saturated dichloromethane (black), ^{12}CO-saturated colloidal solution of $Au_{23}Pd_1$:PVP (red), and DFT-calculated stretching frequencies of ^{12}CO adsorbed on different Au (green) and Pd (blue) sites.

3. Doping and Size Effects on Oxidation Catalysis

The oxidation catalysis of Au_{24}:PVP, $Au_{23}Pd_1$:PVP, and Au_{38}:PVP was investigated by employing aerobic oxidation of benzyl alcohol (**Scheme 1**) as a model reaction. Benzoic acid was the main product and selectivity did not appreciably

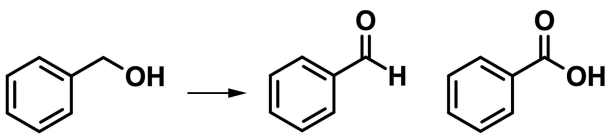

Scheme 1. Aerobic oxidation of benzyl alcohol catalyzed by clusters (solvent: H_2O, base: K_2CO_3).

change depending on the clusters. All the clusters catalyzed the reaction without degradation, as confirmed by optical spectroscopy and MALDI mass spectrometry after reactions. Therefore, the kinetic parameters obtained in this study were intrinsic to the clusters.

Table 1 summarizes the reaction rate constant (k_H) at 303 K, apparent activation energy (E_a) estimated by the Arrhenius plot of k_H as a function of temperature, and kinetic isotope effect (KIE, k_H/k_D) determined using α-deuterated benzyl alcohol ($C_6H_5CD_2OH$). Single Pd atom doping into Au_{24}:PVP significantly increased k_H and reduced E_a. On the other hand, both Au_{24}:PVP and $Au_{23}Pd_1$:PVP showed large KIE values, suggesting that the hydride elimination from the α-carbon of benzyl alcohol by the cluster surface (**Scheme 2**) is rate-determining step. This mechanism was supported by the observation that the reaction rate constant increased with the electron donating ability of substituents at *para*-position. Considering the exposed state of the Pd dopant and high affinity of Pd toward H, it was concluded that the Pd atom acted as a reaction site for hydride elimination with reduced activation energy.

Table 1. Summary of kinetic parameters of the benzyl alcohol oxidation catalyzed by clusters.

Cluster	k_H / h^{-1} [a]	E_a / kJ mol^{-1}	KIE [b]
Au_{24}:PVP	0.83	56 ± 3	4.1
$Au_{23}Pd_1$:PVP	2.3	45 ± 2	3.0
Au_{38}:PVP	1.7	48 ± 1	3.7

[a] Reaction rate constant at 303 K. [b] KIE observed for α-deuterated benzyl alcohol.

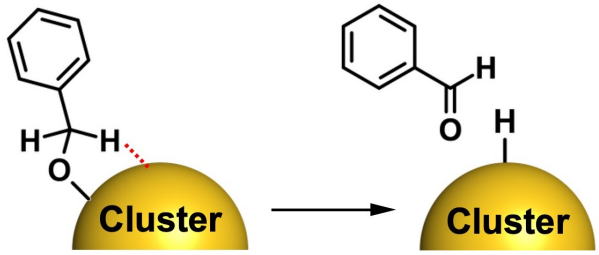

Scheme 2. Hydride elimination step of the catalytic oxidation of benzyl alcohol.

Au_{38}:PVP showed larger k_H and smaller E_a values than those of Au_{24}:PVP, whereas both clusters showed comparable and large KIE (**Table 1**). Catalytic oxidation of *p*-substituted benzyl alcohol by Au_{38}:PVP was promoted by the electron donation by the substituents. Therefore, it was concluded that the hydride elimination step (**Scheme 2**) was also rate-determining for Au_{38}:PVP. Based on the results of DFT calculations in which Au_{38} showed larger adsorption energy of a hydride than that of Au_{24}, it was proposed that the increased affinity to a hydride contributes to the high catalytic activity of Au_{38}:PVP.

4. Conclusion

In my doctoral study, I achieved the atomically precise synthesis of PVP-stabilized Au clusters by kinetic control and size conversion by base treatment to obtain Au_{24}, $Au_{23}Pd_1$, and Au_{38} clusters. ACTEM video imaging revealed the polydispersity and fluxionality of the atomic structures of Au_{24} and Au_{38}. Non-crystalline structures were suggested by DFT calculations and reproduced ACTEM images. Pd K-edge EXAFS, FT-IR spectroscopy, and DFT calculations indicated that the Pd atom of $Au_{23}Pd_1$ was located on the cluster surface. These clusters catalyzed the aerobic oxidation of benzyl alcohol without degradation and it was found that the single Pd atom doping and size increase significantly enhanced the catalytic activity. Kinetic studies indicated that the increased catalytic activities were ascribed to the promotion of rate-determining hydride elimination step.

References

[1] Jin, R.; Zeng, C.; Zhou, M.; Chen, Y. *Chem. Rev.* **2016**, *116*, 10346. [2] Liu, L.; Corma, A. *Chem. Rev.* **2018**, *118*, 4981. [3] Omoda, T.; Takano, S.; Tsukuda, T. *Small* **2021**, *17*, 2001439. [4] Hasegawa, S.; Tsukuda, T. *Bull. Chem. Soc. Jpn.* **2021**, *94*, 1036. [5] Yamazoe, S.; Koyasu, K.; Tsukuda, T. *Acc. Chem. Res*. **2014**, *47*, 816.